Triple coupling and parameter resonance in quantum optomechanics with a single atom

2009 J. Phys. B: At. Mol. Opt. Phys. 42 215502

(http://iopscience.iop.org/0953-4075/42/21/215502)

J. Phys. B: At. Mol. Opt. Phys. **42** (2009) 215502 (9pp) doi:10.1088/0953-4075/42/21/215502

Triple coupling and parameter resonance in quantum optomechanics with a single atom

Yue Chang, H Ian and C P Sun

Institute of Theoretical Physics, Chinese Academy of Sciences, Beijing, 100190, People's Republic of China

E-mail: suncp@itp.ac.cn

Received 13 July 2009, in final form 11 September 2009
Published 14 October 2009
Online at stacks.iop.org/JPhysB/42/215502

Abstract

We study the energy level structure and quantum dynamics for a cavity optomechanical system assisted by a single atom. It is found that a triple coupling involving a photon, a phonon and an atom cannot be described only by the quasi-orbital angular momentum at frequency resonance, there also exists the phenomenon of parameter resonance, namely, when the system parameters are matched in some way, the evolution of the end mirror of the cavity is conditioned by the dressed states of the photon–atom subsystem. The quantum decoherence due to this conditional dynamics is studied in detail. In the quasi-classical limit of very large angular momentum, this system will behave like a standard cavity-QED system described by the Jaynes–Cummings (J–C) model when the angular momentum operators are transformed to bosonic operators of a single mode. We test this observation with an experimentally accessible parameter.

1. Introduction

Nowadays, there is an increasing number of researches on cavity optomechanical systems assisted by atoms or atomic ensembles [1–3]. Such hybrid systems show a convergence between quantum optics and nano(micro)-mechanical systems. Furthermore, novel quantum natures are discovered in this composite system by placing atoms confined in a gas chamber inside the cavity. With the help of the atoms, theoretical explorations have been made to show the possibilities to create not only the entanglement between the cavity field and a macroscopical object [4–7], i.e., a mirror, but also the entanglement of an atom and a light mirror [1,3].

In this paper, we will further study this atom-assisted optomechanical (AAOPM) system with the strong coupling of a single atom to the photon field inside the cavity, which is modified by the moving end mirror of the cavity (see figure 1). A three-body coupling term of a photon, a phonon and an atom will play the crucial role in the quantum dynamics of the triple system. This triple coupling was also given in [8], where the authors studied the effect of this term on the atomic population evolution. Our present emphasis is placed on the different physical phenomena due to this triple coupling. For example, the parametric resonance happens as a matching condition concerning the frequencies and the coupling strength. The present investigation substantially consolidates our previous series studies (see [3], for example) on quantum optomechanics with this finding about triple coupling.

The triple system we will refer to contains a two-level system interacting with a single-mode electromagnetic field inside the cavity with an oscillating mirror. We emphasize the case that the atom is fixed in the cavity. In this case, we can use an artificial atom (such as SQUIDs [9]) as the two-level system, then the motion of the mass-center of the atom can be ignored, and the strong coupling region can be reached easily. Due to the vibration of the cavity length, which is conventionally thought to induce the radiation pressure term [7,10–12], we illustrate that the vibrating length can also result in the triple coupling term of the photon, atom and mirror, and the triple coupling cannot be neglected in the strong coupling region. When the parameters of the system, i.e., the frequencies and the coupling strengths, are matched in some way, namely, they satisfy the so-called parametric resonance condition, we can exactly diagonalize the Hamiltonian. In this case, the evolution of the end mirror is determined by the conditional

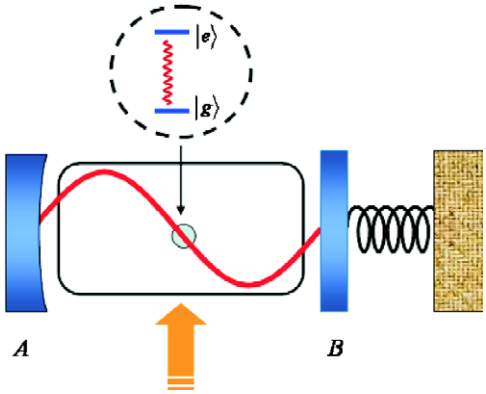

Figure 1. The schematic of the atom-assisted optomechanical (AAOPM) system. It contains an optical cavity ended with a fixed mirror A and a slightly moving mirror B which is attached to a spring. Inside the cavity there is a two-level atom.

Hamiltonian concerning different dressed states of the photon–atom subsystem. We consider how the mirror's oscillation affects the cavity-QED subsystem, by studying the quantum decoherence [13] of this subsystem.

The above condition for exact solution seems too special to be realized, thus we subsequently consider a more general case with the rotating-wave approximation, which loses the requirement for exact solution to a set of matching frequencies only, among the atom, the cavity field and the mirror. In this case, our model is reduced to the generalized spin–orbit coupling model where the spin is referred to as the internal energy level of the atom, while the orbit is depicted by the quasi-orbital angular momentum defined by two bosonic modes (the mirror oscillation and the single-mode photon of the cavity) through the Jordan–Schwinger representation.

It is well known that the quantum system with a large angular momentum L can be regarded as a classical rotor when the angular momentum approaches infinity in the classical limit [15] because the component variations ΔJ_x, ΔJ_y and ΔJ_z become vanishingly small in comparison with the large angular momentum L. When the angular momentum is large enough, but not infinite, the ladder operators of any large angular momentum can behave as the creation and annihilation operators of a single-mode boson [16,17]. This point can be seen from the Holstein–Primakoff transformation straightforwardly. This case is named the quasi-classical limit and its significance in many-body physics can be understood as the low-energy excitation above the ordered ground states. This quasi-classical reduction of large angular momentum has extensively been studied and applied in quantum storage [18–20]. Here, we study this quasi-classical reduction in this triple system. When the frequency resonance condition is satisfied, our triple system is modelled by the generalized spin–orbit coupling similar to the Hamiltonian for the Paschen–Back effect without the radial dependence [21]. This observation means that the triple coupling system will be reduced to a two-part coupling system described by the Jaynes–Cummings (J–C) model in cavity QED. Finally, we show this quasi-classical reduction indeed works well when the hybrid excitation of the mirror plus photon is large enough.

The paper is organized as follows. In section 2, we model the AAOPM coupling and reduce it to the generalized spin–orbit coupling under the frequency matching condition. In section 3, we exactly solve the AAOPM model under the parametric resonance condition and show the decoherence in section 4. In section 5, we compare the generalized spin–orbit coupling model with the J–C model by their eigenstates and eigenvalues. Furthermore, in section 6, we study the dynamics of the generalized spin–orbit coupling model to demonstrate its similarities to and differences from that of the J–C model. In section 7, we summarize our results.

2. Triple coupling of the atom, photon and mirror, and its quasi-orbital description

In this section, we study an experimentally accessible AAOPM system, as illustrated in figure 1. This system consists of three parts: an atom (actually an artificial atom such as the Cooper pair box), photons inside a cavity, and a movable end mirror. As one of the central results, it will be proved that such a hybrid system can be modelled by a spin–orbit coupling system, where the orbital angular momenta are realized by the phonon of the mirror dressed by the photon of the light field inside the cavity. In certain situations, this model has even been studied by us [3] and others [1]. But in this paper, we will emphasize the different emerging phenomena due to the triple interaction in the strong coupling region.

The single-mode electric field inside the cavity along the x-axis is quantized as

$$E(x_0) = \varepsilon a \sin kx_0 + \text{h.c.}, \tag{1}$$

where x_0 is the position of the atomic center of mass, $\varepsilon = \sqrt{\omega_0/\epsilon_0 V}$, and a is the annihilation operator of the oscillating mode of the cavity field. The frequency of the cavity field is dependent on the cavity length, $\omega_0 = k = 2\pi/l_0$, ϵ_0 is the dielectric constant in vacuum, l_0 and V are the length and the volume of the cavity, respectively. Here, we omit the polarization of the field, but this will not affect our final conclusion for a practical system. When the length of the cavity slightly changes from l_0 to $l_0 + x$ due to the mirror's displacement x (see figure 2), the electric field becomes

$$E(x_0) \approx \varepsilon a \sin kx_0 - \eta' x a + \text{h.c.}, \tag{2}$$

where $\eta' = (\sin kx_0 + kx_0 \cos kx_0)\varepsilon/l$ (see the appendix).

As we mentioned in the introduction, we need not consider the motion of the atom when we can use the artificial atom, such as the Cooper pair box or other superconducting qubit, as the two-level system. Then, the total Hamiltonian reads

$$\begin{aligned} H &= \frac{2\pi}{l} a^\dagger a + \omega_M b^\dagger b + \omega_e S_z - [\mu E(x_0) S_+ + \text{h.c.}] \\ &\approx \omega_0 a^\dagger a + \omega_M b^\dagger b - \xi\left(b + b^\dagger\right) a^\dagger a + \omega_e S_z \\ &\quad + \left[g a S_+ + \eta\left(b + b^\dagger\right) a S_+ + \text{h.c.}\right], \end{aligned} \tag{3}$$

where $b^\dagger$ is the creation operator of the oscillating mode of the mirror, S_z, S_+ and S_- are the spin operators, which represent the transitions among the atomic inner states, and ω_e is the difference between the energy levels of the two

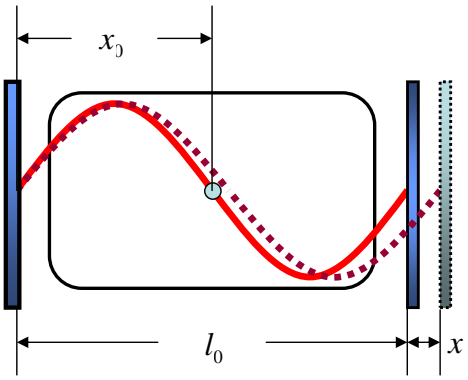

Figure 2. Schematic of the origin of the triple coupling. When the length of the cavity oscillates, besides the light pressure term, the displacement of the mirror will affect the coupling strength between the atom and the light. The triple coupling term appears with this.

atomic inner states. $g = -\mu\varepsilon \sin kx_0$ is the atomic-position-dependent coupling strength between the cavity field and the atom, where μ is the electric-dipole transition matrix element. $\xi = \omega_0/l_0\sqrt{2M\omega_M}$ describes the radiation pressure, where ω_M is the frequency of the mirror's oscillation, and M is the mass of the mirror, while $\eta = \eta'\mu/\sqrt{2M\omega_M}$ denotes the coupling strength of the 'three bodies' due to the vibration of the mirror. Here, we have expanded the first and last two terms of the first line in equation (3) to the first order of x/l_0, just as we do in the appendix, and we have applied the rotating-wave approximation to neglect the terms containing aS_- and its Hermitian conjugate.

With experimentally feasible parameters, there exists the situation where η is of the same order of magnitude as ξ, for which the strong coupling region [23–25] is reached (e.g., $g = \omega_0 = 10^{15}$ Hz and $kx_0 = \pi/2$, then $\eta = -\xi$). We note that this strong coupling region can be reached in current experiments [25] in semiconductor quantum wells, where Plumridge *et al* used a semiconductor-based quantum metamaterial as a collection of artificial atoms and found that the coupling between the light and the artificial atom can reach the 'ultra-strong-coupling' region. In this region, the coupling strength and the frequency of the light are comparable. In this case, i.e., when the coupling strength is so strong that it is comparable with the cavity frequency, the triple coupling term,

$$V_T = \eta\left(b + b^\dagger\right)a\,|e\rangle\langle g| + \text{h.c.}, \tag{4}$$

should not be neglected. In the following discussion, we focus on this strong coupling case.

It follows from the Hamiltonian in equation (3) that, when $\sin kx_0 \to 0$, i.e., $g \to 0$, the J–C type interaction $gaS_+ + \text{h.c.}$ vanishes, but the three-body interaction remains. Near the photon–phonon resonance case where the frequencies satisfy $\omega_e + \omega_M - \omega_0 \approx 0$, the rotating-wave approximation reduces the Hamiltonian to

$$H_{\text{RWA}} = \omega_0 a^\dagger a + \omega_M b^\dagger b + \omega_e S_z + \eta\left(b^\dagger a S_+ + \text{h.c.}\right). \tag{5}$$

In the following discussions, we invoke the Jordan–Schwinger representation of the $SO(3)$ group [22]:

$$L_+ = a^\dagger b, \qquad L_- = ab^\dagger, \qquad L_z = \frac{1}{2}\left(a^\dagger a - b^\dagger b\right), \tag{6a}$$

where the commutation relations of the angular momenta

$$[L_+, L_-] = 2L_z, \quad [L_z, L_+] = L_+, \quad [L_z, L_-] = -L_- \tag{6b}$$

are satisfied due to the generic commutation relations between the bosonic operators a and b. Then, the Hamiltonian can be rewritten as

$$H_{\text{RWA}} = \Omega N + \kappa L_z + \omega_e S_z + \eta(L_- S_+ + L_+ S_-), \tag{7}$$

where $N = a^\dagger a + b^\dagger b$, $\Omega = (\omega_0 + \omega_M)/2$ and $\kappa = \omega_0 - \omega_M$.

We remark that the three-body interaction in the AAOPM system can be approximately modelled with the x–y coupling:

$$\eta(L_- S_+ + L_+ S_-) = 2\eta\left(L_x S_x + L_y S_y\right). \tag{8}$$

This is a kind of 'spin–orbit coupling' referred to as the Paschen–Back effect [21]. The 'orbital' angular momentum defined by $L_\pm$ and L_z essentially results from the joint excitation of the photon and the phonon. Physically, this excitation can be understood as a kind of effective mechanical oscillation of the mirror, which is dressed by the single-mode photon. Such kinds of dressed bosons satisfy the angular momentum algebra.

3. Parametric resonance

In this section, we show the parametric resonance phenomenon results in a conditional dynamics of the triple coupling system. Namely, when the parameters of the system are matched in some way, the cavity-QED subsystem is confined in the subspace with total excitations so that its state determines time evolution of the end mirror.

Now let us temporarily leave the above concrete system to consider a more general spin–boson system with the Hamiltonian of the form

$$H_{\text{SP}} = h\left(b, b^\dagger\right) + W\left(S; b, b^\dagger\right), \tag{9}$$

where $h\left(b, b^\dagger\right)$ is a function that only depends on the boson model, and $W\left(S; b, b^\dagger\right)$ is spin dependent where S represents the spin variable. There is a seemingly trivial proposition for this spin–boson system: if the system parameters are matched so that the coupling can be factorized as

$$W\left(S; b, b^\dagger\right) = f\left(b, b^\dagger\right)M(S), \tag{10}$$

with $f\left(b, b^\dagger\right)$ $(M(S))$ depending on the boson (spin) only, then H_{SP} can be exactly diagonalized through the diagonalizations of the two pure boson systems with branch Hamiltonians

$$H_{\text{SP}}^{\pm} = h\left(b, b^\dagger\right) + \lambda^{\pm} f\left(b, b^\dagger\right), \tag{11}$$

where λ^+ and λ^- are the eigenvalues of the C-number coefficient matrix $M(S)$ in the basis $\{|+\rangle\,,\ |-\rangle\}$ which make $M(S)$ diagonalized. The proof of the above observation is rather straightforward and we only need to diagonalize $M(S)$ first. Essentially, equations (9) and (11) describe a conditional dynamics determined by the conditional Hamiltonian $H_{\text{SP}}^{(+)}$ or $H_{\text{SP}}^{(-)}$ which is the diagonal element of H_{SP} in the basis $\{|+\rangle\,,\ |-\rangle\}$.

Next, we return to the concrete example. From equation (3), obviously the particle number operator $N = a^\dagger a + S_z$ is conserved, i.e., $[N, H] = 0$. Then, in the subspace

$\{|n_a+1,g\rangle,\ |n_a,e\rangle\}$, $|n_a,g(e)\rangle$ denotes that the photon is prepared in a Fock state $|n_a\rangle$ while the atom in the ground (excited) state. We consider the situation in which the eigenequation of the Hamiltonian in equation (3) can be solved exactly. To this end, we first show that the Hamiltonian is formally expanded as follows:

$$H_{n_a} = h\left(b,b^\dagger\right) + H'_{n_a}, \tag{12}$$

where

$$h\left(b,b^\dagger\right) = \omega_e + \omega_0 n_a + \omega_M b^\dagger b - \xi n_a\left(b+b^\dagger\right) \tag{13}$$

and

$$H'_{n_a} = \sqrt{n_a+1}\begin{pmatrix} \frac{\Delta-\xi\left(b+b^\dagger\right)}{\sqrt{n_a+1}} & g-\eta\left(b+b^\dagger\right) \\ g-\eta\left(b+b^\dagger\right) & 0 \end{pmatrix}. \tag{14}$$

In equation (14), $\Delta=\omega_0-\omega_e$ is the atom–photon detuning. The above argument shows that in the subspace the total system can be reduced to a spin–boson model defined by equations (12)–(14).

We explore the condition when H'_{n_a} can be factorized to $f\left(b,b^\dagger\right)M_{n_a}$, where $f\left(b,b^\dagger\right)$ is a function of b and $b^\dagger$, and M_{n_a} is a C-number matrix. Actually, when the detuning Δ and the three coupling coefficients satisfy the relation

$$g\xi = \Delta\eta, \tag{15}$$

which we call the parametric resonance, the Hamiltonian indeed becomes the form of equation (10):

$$H_{n_a} = h\left(b,b^\dagger\right) + f\left(b,b^\dagger\right)M_{n_a}, \tag{16}$$

where

$$f\left(b,b^\dagger\right) = \Delta - \xi\left(b+b^\dagger\right), \tag{17}$$

and

$$M_{n_a} = \begin{pmatrix} 1 & \sqrt{n_a+1}\eta/\xi \\ \sqrt{n_a+1}\eta/\xi & 0 \end{pmatrix}. \tag{18}$$

Thus, to diagonalize the Hamiltonian H_{n_a}, all we need to do is to diagonalize the matrix M_{n_a} and the left quadratic part formed by b and $b^\dagger$. Then, the eigenvalues of H are obtained as

$$E_{j,n_a,n_b} = \omega_0\left(n_a+\frac{1}{2}\right)+\frac{1}{2}\omega_e+\frac{(-)^j}{2}R_{n_a}\Delta + n_b\omega_M - \alpha^2_{jn_a}, \tag{19a}$$

for $j=1,2$, where

$$R_{n_a} = \sqrt{1+\frac{4\eta^2(n_a+1)}{\xi^2}}, \tag{19b}$$

and

$$\alpha_{jn_a} = \frac{\xi}{2\omega_M}\left(2n_a+(-)^j R_{n_a}+1\right). \tag{19c}$$

Here, n_a (n_b) represents the quantum number of the photons (phonons). Correspondingly, the eigenstates of the AAOPM system are $|jn_a\rangle\otimes|n_b\rangle_{jn_a}$, where the photon dressed states

$$|1n_a\rangle = \cos\theta_{n_a}|n_a+1,g\rangle + \sin\theta_{n_a}|n_a,e\rangle, \tag{20a}$$

and

$$|2n_a\rangle = -\sin\theta_{n_a}|n_a+1,g\rangle + \cos\theta_{n_a}|n_a,e\rangle, \tag{20b}$$

are defined by the mixing angle θ_{n_a}:

$$\tan\theta_{n_a} = \frac{2\eta\sqrt{n_a+1}}{\xi-\xi R_{n_a}}, \tag{21}$$

while the mirror's states $|n_b\rangle_{jn_a}$ are

$$|n_b\rangle_{jn_a} = \frac{1}{\sqrt{n_b!}}\left(b^\dagger-\alpha_{jn_a}\right)^{n_b} D_b\left(\alpha_{jn_a}\right)|0\rangle, \tag{22}$$

with the displacement operator $D_b\left(\alpha_{jn_a}\right) = \exp\left[\alpha_{jn_a}\left(b^\dagger-b\right)\right]$.

If $\xi=\eta=0$, the AAOPM coupling model reduces back to the J–C model, and the eigenvalues, together with the eigenstates, degenerate to that of the J–C model. However, due to the vibration of the mirror, there emerge fruitful results in our model due to the complex three-body coupling. First, we examine the realization of the parametric resonance condition, equation (15), in experiments [25, 27, 28]. Substituting the experimental feasible parameters into the parametric resonance condition, we know that it is easily satisfied if the detuning Δ is adjusted properly to adapt to different positions of the atom. In experiments, ξ and η can reach 10^5 Hz, while g is on the order of 10^{15} Hz, thus Δ can be on any order that lies on the atomic position. In the special case when $\sin kx_0=0$, i.e., $g=0$, $\Delta=0$ is sufficient to meet the condition in equation (15).

It is observed from equation (19*a*) that the terms in the second line obviously differ from the eigenvalues of the J–C model. The first term is the mirror's eigenvalue, and the second one (without the sign) is expanded as

$$\frac{\xi^2 n_a^2}{\omega_M}+\frac{\xi^2}{4\omega_M}\left(4n_a+(-)^j R_{n_a}+1\right)\left((-)^j R_{n_a}+1\right), \tag{23}$$

where the first term $\xi^2 n_a^2/\omega_M$ describes the energy of the light pressure term $\xi\left(b+b^\dagger\right)a^\dagger a$ [6,26], but the left terms are induced by the AAOPM coupling.

4. Conditional dynamics for decoherence

In this section, we demonstrate that the parametric resonance will lead to a conditional dynamics with respect to two superpositions of atomic inner states $|+\rangle$ and $|-\rangle$, which is described by a non-demolition Hamiltonian.

From the above argument about the exact solvability of the AAOPM system, we can find that the operator-valued Hamiltonian matrix

$$H = \begin{bmatrix} H_{\rm SP}^{(+)} & 0 \\ 0 & H_{\rm SP}^{(-)} \end{bmatrix} \tag{24}$$

is diagonalized with respect to the bases $\{|+\rangle,\ |-\rangle\}$ for the spin part. Obviously, this is a non-demolition Hamiltonian with respect to the basis vectors $|+\rangle$ and $|-\rangle$,and thus results in the corresponding decoherence.

Driven by this non-demolition Hamiltonian, the factorized initial state for the cavity-QED system

$$|\psi(0)\rangle = (C_+|+\rangle + C_-|-\rangle)\otimes|\varphi\rangle \tag{25}$$

will evolve into an entanglement state

$$|\psi(t)\rangle = C_+|+\rangle|\varphi_+(t)\rangle + C_-|-\rangle|\varphi_-(t)\rangle, \tag{26}$$

where

$$|\varphi_{\pm}(t)\rangle = \mathrm{e}^{-\mathrm{i}H_{\mathrm{SP}}^{(\pm)}t}\,|\varphi\rangle\,,$$

and the extent of decoherence due to this quantum entanglement is characterized by the so-called decoherence factor

$$\begin{aligned} D(t) &= \langle\varphi_{+}(t)\,|\varphi_{-}(t)\rangle \\ &= \mathrm{Tr}\left(\rho(0)\mathrm{e}^{\mathrm{i}H_{\mathrm{SP}}^{(+)}t}\mathrm{e}^{-\mathrm{i}H_{\mathrm{SP}}^{(-)}t}\right), \end{aligned} \tag{27}$$

and its norm square $L(t) = |D(t)|^2$ is the so-called Loschmidt echo (LE)[14].

In the context of quantum chaos, the LE characterizes the sensitivity of evolution of the quantum system in comparison with the butterfly effect in classical chaos: starting from the same initial state, the quantum system is separately driven by two slight different Hamiltonians. Quantum chaos is implied by the much larger differences in the two corresponding final states; namely, their overlap (LE) vanishes to illustrate the dynamical sensitivity of the quantum chaos system.

Next we return to the concrete system.

Consider the time evolution of the system when the initial state is as follows:

$$\psi(0) = \sum_{j,n_a}\lambda_{jn_a}\,|jn_a\rangle\otimes|\beta\rangle_b\,, \tag{28}$$

where $|\beta\rangle_b$ is a coherent state of a phonon that satisfies

$$b\,|\beta\rangle_b = \beta\,|\beta\rangle_b\,, \tag{29}$$

$|jn_a\rangle$, $j = 1, 2$, is the dressed state mentioned in the last section, and λ_{jn_a} is the weight of each dressed state. Therefore, at time t the wavefunction of the total system is

$$\psi(t) = \sum_{j,n_a}\lambda_{jn_a}\,|jn_a\rangle\otimes\mathrm{e}^{-jC_{jn_a}t}\left|\left(\beta-\alpha_{jn_a}\right)\mathrm{e}^{-j\omega_M t}+\alpha_{jn_a}\right\rangle_b \tag{30}$$

where

$$\begin{aligned} C_{jn_a} &= \frac{1}{2}\omega_e + \omega_0\left(n_a+\frac{1}{2}\right) + \frac{(-)^j}{2}R_{n_a}\Delta \\ &\quad - \frac{\xi^2}{4\omega_M}\left(2n_a + (-)^j\,R_{n_a}+1\right)^2. \end{aligned} \tag{31}$$

The mirror's motion will result in the collapse of the decoherence, with the LE being

$$\begin{aligned} \mathrm{LE}_{n_a,m_a}^{j_1,j_2} &= \left|{}_b\langle\beta|\,\mathrm{e}^{\mathrm{i}H_{j_2n_a}t}\mathrm{e}^{-\mathrm{i}H_{j_1m_a}t}\,|\beta\rangle_b\right|^2 \\ &= \exp\left[2\left(\Delta_{n_a,m_a}^{j_1,j_2}\right)^2(\cos\omega_M t-1)\right], \end{aligned} \tag{32}$$

where

$$\Delta_{n_a,m_a}^{j_1,j_2} = \alpha_{in_a} - \alpha_{jm_a}. \tag{33}$$

We note that β does not play any role in the LE. Note that the mirror's initial coherent state evolves to another coherent state, and β only determines the initial position of the center of the wavepacket $\langle x\,|\beta\rangle_b$. Thus the overlap of the two wavepackets $\exp(-\mathrm{i}H_{j_1n_a}t)\,|\beta\rangle_b$ and $\exp(-\mathrm{i}H_{j_2m_a}t)\,|\beta\rangle_b$ is independent of β. Physically, this fact shows that the decoherence of the cavity-QED system is irrelevant to the phonon excitations of the mirror if its wavepacket is Gaussian.

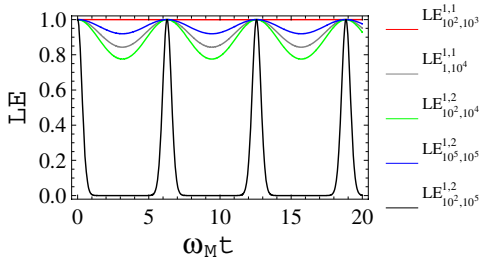

Figure 3. The time evolution of the Loschmidt echo (LE) with different indices of LE as shown in the equations above, which correspond to photon–phonon excitations.

In figure 3, for different photon–phonon excitations, we plot the time evolution of the LE with the parameters set to $\omega_0 = 10^{15}$ Hz, $\eta = 10\omega_0/l\sqrt{2M\omega_M} = 10\xi$, $l_0 = 1\mu$m, $M = 10^{-10}$ kg, $\omega_M = 10^9$ Hz. From figure 3, we see that all the curves have the same period, i.e., $2\pi/\omega_M$, and the larger the difference of the photon number $|n_a - m_a|$, the larger the amplitudes of the curve. We remark that the large photon number means a classical electromagnetic field, and thus the quantum decoherence of the atomic inner states reflects the classical transition of optical field from the quantum regime.

5. Modelling frequency resonance with the generalized Jaynes–Cummings model

In this section, we will study the relations between the J–C model and the model above with generalized spin–orbital coupling in the quasi-classical limit.

5.1. Jordan–Schwinger representation of the triple coupling model

In section 2, we have derived the generalized spin–orbit coupling model under the rotating-wave approximation, which can be rewritten as

$$H_{\mathrm{RWA}} = \Omega N + \kappa L_z + \omega_e S_z + 2\eta\left(\vec{L}\cdot\vec{S} - L_z S_z\right), \tag{34}$$

where κ and ω_e characterize the coupling of the angular momentum and the spin to the external field, respectively, 2η is the coupling strength of the spin–orbit.

This model can be studied by exactly diagonalizing the model Hamiltonian in equation (34) within its invariant subspace spanned by

$$|l, m, e\rangle = |l, m\rangle\otimes|\uparrow\rangle \tag{35a}$$

and

$$|l, m+1, g\rangle = |l, m+1\rangle\otimes|\downarrow\rangle\,. \tag{35b}$$

Here, $|l, m\rangle$ is the standard angular momentum basis, while $|\uparrow\rangle$ and $|\downarrow\rangle$ denote the spin-up and spin-down vectors, respectively. In this basis, the spin–orbit coupling Hamiltonian in equation (34) is reduced to a quasi-diagonal matrix with an 2×2 block:

$$H_{\mathrm{RWA}}^{l} = 2\Omega l + \left(m+\frac{1}{2}\right)\delta + \frac{1}{2}\begin{pmatrix}\delta & g_{lm}\\ g_{lm} & -\delta\end{pmatrix}, \tag{36}$$

where $\Delta = \omega_e - \delta$,and

$$g_{lm} = 2\eta\sqrt{l\,(l+1) - m\,(m+1)}. \tag{37}$$

Then it can be further diagonalized to obtain the eigenvectors

$$|+lm\rangle = \cos\theta_{lm}\,|l, m, e\rangle + \sin\theta_{lm}\,|l, m+1, g\rangle \qquad (38a)$$

and

$$|-lm\rangle = -\sin\theta_{lm}\,|l, m, e\rangle + \cos\theta_{lm}\,|l, m+1, g\rangle\,, \qquad (38b)$$

with the corresponding eigenvalues

$$E_{\pm lm} = 2\Omega l + \left(m + \frac{1}{2}\right)\kappa \pm \frac{1}{2}R_{lm}, \qquad (39)$$

where $\tan\theta_{lm} = g_{lm}/(\delta + R_{lm})$ and $R_{lm} = \sqrt{g_{lm}^2 + \delta^2}$.

From the spectrum structure of the AAOPM system described above, we demonstrate that the triple coupling system can realize the entanglement between an orbital angular momentum and a spin. The z-component of the total angular momentum is conserved. Thus, while the orbital angular momentum is flipped from down (up) to up (down), the spin will make a reverse flip.

5.2. *Quasi-classical limit*

Now we can consider the quasi-classical limit of the above spin–orbit coupling model for l large enough with low excitation. Obviously, the above basis vector in this limit becomes a Fock state, i.e., $|l, m\rangle \to |n\rangle$, where $n = l + m$, $n/l \ll 1$; while $\tan\theta_{lm} \to \tan\theta_n = g_n/(\delta + R_n)$. Correspondingly, the eigenstates become the dressed states in the usual J–C model with the eigenvalues

$$E_{\pm lm} \to E_{\pm n} = \left(n + \frac{1}{2}\right)\kappa \pm \frac{1}{2}R_n, \qquad i = 1, 2, \qquad (40)$$

where $g_n = 2\eta\sqrt{2l\,(n+1)}$ and $R_n = \sqrt{g_n^2 + \delta^2}$.

We remark that the system we considered in the limit above can also be described by the J–C model:

$$H_{\mathrm{J-C}} = \kappa a^\dagger a + \omega_e S_z + \eta\sqrt{2l}\left(aS_+ + a^\dagger S_-\right). \qquad (41)$$

The correspondence between the Fock state $|n\rangle$ and the standard angular momentum basis is

$$|n\rangle \Leftrightarrow |l, l-n\rangle\,. \qquad (42)$$

Actually, the above equivalence of spin–orbit coupling model and J–C interaction can be found directly by considering the Holstein–Primakoff mapping,

$$L_+ = a^\dagger\sqrt{2l - a^\dagger a}, \quad L_- = L_+^\dagger, \quad L_z = a^\dagger a - l \qquad (43)$$

in the large l limit.

Next we come back to the practical physics of the AAOPM system. Then the joint states $|l, m, e\,(g)\rangle = |l, m\rangle \otimes |\uparrow\,(\downarrow)\rangle$ is re-expressed in terms of the two Fock states $|l+m\rangle_a$ and $|l-m\rangle_b$ as

$$|l, m, e\,(g)\rangle = |l+m\rangle_a\,|l-m\rangle_b\,|e\,(g)\rangle\,. \qquad (44)$$

Here $|l+m\rangle_a$ and $|l-m\rangle_b$ represent the states with $l+m$ photons and $l-m$ phonons of the mirror's vibration mode, respectively.

In figures 4 and 5, with different values of l and m, we plot $E_{\pm lm}$ as functions of ω_e. Here, we take the physical parameters as $\omega_0 = 1.9 \times 10^{15}$ Hz, $\eta = \omega_0/l\sqrt{2M\omega_M}$, $l_0 = 1\,\mu$m, $M = 10^{-10}$ kg, $\omega_M = 10^9$ Hz. As shown in figures 4 and 5, when l is fixed, the spectrum diagram of the AAOPM system looks quite like that of the J–C model's [29]. However, in general, its number of energy levels is much more than that in the J–C model's within the same energy range. Furthermore, we can see from the several lowest levels that there exist small differences under different values of l, such as $E_{+,1,-1}$ versus $E_{+,1000,-1000}$, $E_{-,1,0}$ versus $E_{-,1000,-999}$ and so on. Accordingly, the larger the value of l (the orbital angular momentum), the closer the spectrum is to the corresponding ones in the J–C model. For evidence, we have plotted the curves with a much larger range of the variable ω_e that is not valid in our rotating-wave approximation that requires $|\omega_e - \omega_0| \ll \omega_M$.

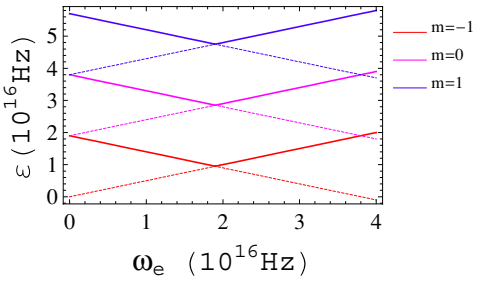

Figure 4. Schematic of the relation of the eigenvalues of the atom–photon–mirror coupling system with the spacing frequency of the two-level atom. Here we take $m = -1, 0, 1$ when l=1. Each real line represents ε_{+lm} while the dashed with the same color represents ε_{+lm}.

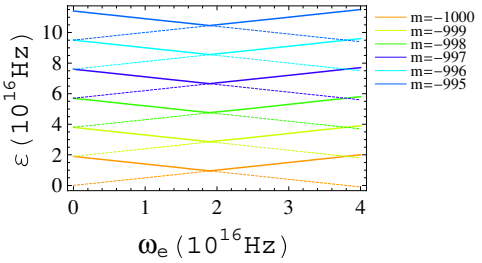

Figure 5. Schematic of the lowest 5 levels when l=1000.

6. Quasi-classical dynamics

In the above sections, we have shown the similarity between the triple hybrid system and the J–C model in their energy spectra. Now we continue to consider this similarity in quantum dynamics, which is referred to as the so-called quasi-classical one as we make the analysis for very large angular momentum.

We consider that generally the system described by the Hamiltonian equation (34) is initially prepared in the state represented by the density matrix

$$\rho\,(0) = \sum_{ijkl}\lambda_{ij;kl}\left|\psi_{ij}\,(0)\right\rangle\langle\psi_{kl}\,(0)|\,, \qquad (45)$$

where the joint states $\left|\psi_{ij}\,(0)\right\rangle = |i\rangle_a\,|j\rangle_b\,|e\rangle$ denote the initial factorized structure of the triple system. According to the similarity between the generalized L–S coupling system and

the triple coupling system we mentioned in the last section, the density matrix for the time evolution reads

$$\rho(t) = \sum_{ijkl} \lambda_{ij;kl} \left|\psi_{ij}(t)\right\rangle \left\langle\psi_{kl}(t)\right|, \tag{46}$$

where the branch wavefunctions

$$\begin{aligned}\left|\psi_{ij}(t)\right\rangle = \mathrm{e}^{-\mathrm{i}\omega_{ij}t}[\lambda^{e}_{ij}(t)\left|i\right\rangle_a\left|j\right\rangle_b\left|e\right\rangle \\ -\lambda^{g}_{i+1,j-1}(t)\left|i+1\right\rangle_a\left|j-1\right\rangle_b\left|g\right\rangle],\end{aligned} \tag{47}$$

for $\omega_{ij} = \omega_0 i + \omega_M j + \delta/2$, are determined by the time-dependent parameters defined by

$$\lambda^{e}_{ij}(t) = \cos\frac{\Omega_{ij}t}{2} - \mathrm{i}\cos 2\phi_{ij}\sin\frac{\Omega_{ij}t}{2}, \tag{48a}$$

$$\lambda^{g}_{i+1,j-1}(t) = \mathrm{i}\sin 2\phi_{ij}\sin\frac{\Omega_{ij}t}{2}, \tag{48b}$$

$$\tan\phi_{ij} = \frac{2\eta\sqrt{j(i+1)}}{\omega_e - \delta + \Omega_{ij}}, \tag{48c}$$

$$\Omega_{ij} = \sqrt{4\eta^2[j(i+1)] + (\omega_e - \delta)^2}. \tag{48d}$$

It is noted that the above equations (47)–(48*d*) have forms similar to that for the J–C model in the limit that $i/j \ll 1$. We remark that this limit means a low excitation of the joint system consisting of the photon and phonon, i.e., there are only a few photons stimulated so that the joint system is almost prepared in the lowest weight state $|l, m = -l\rangle$. The above equations give us rich information on the complex system, from which all the physically relevant quantities to the cavity field, the atom and the mirror can be obtained. In equation (47), $\left|\lambda^{e}_{ij}(t)\right|^2$ $\left(\left|\lambda^{g}_{ij}(t)\right|^2\right)$ is proportional to the probability that at time t, there are i photons, j quanta of the mirror's vibration mode and one atom in the excited (ground) state. Therefore, the probability $p_n(t)$ that n photons are measured is

$$\begin{aligned}p_n(t) = \sum_j \lambda_{nj;nj}\left(c^2_{nj}(t) + \cos^2 2\phi_{nj}s^2_{nj}(t)\right) \\ + \left|\lambda_{n-1,j;n-1,j}\right|^2 \sin^2 2\phi_{n-1,j}s^2_{n-1,j}(t),\end{aligned} \tag{49}$$

where $c_{nj}(t) = \cos\Omega_{nj}t/2$ and $s_{nj}(t) = \sin\Omega_{nj}t/2$.

Another important quantity is the population inversion $W(t)$ depending on the probability amplitudes $\lambda^{e}_{ij}(t)$ and $\lambda^{g}_{ij}(t)$ as

$$\begin{aligned}W(t) &= \sum_{i,j}\lambda_{ij;ij}\left(\left|\lambda^{e}_{ij}(t)\right|^2 - \left|\lambda^{g}_{i+1,j-1}(t)\right|^2\right) \\ &= \sum_{i,j}\lambda_{ij;ij}[c^2_{ij}(t) + \cos 4\phi_{ij}s^2_{ij}(t)].\end{aligned} \tag{50}$$

Note that if the initial state of the mirror is the vacuum state, i.e., $\lambda_{ij;kl} \propto \delta_{j0}\delta_{l0}$, then it follows from equations (49) and (50) that $p_n(t) = \sum_j \lambda_{nj;nj}$ and $W(t) = 1$, both of which are time independent no matter which state the light field is initially in. This result can be explained as follows: with the rotating-wave approximation, we only hold the slowly-varying terms in the original Hamiltonian to obtain effective Hamiltonian (5). These terms make a transition from the atom's upper level state $|e\rangle$ to the ground state $|g\rangle$, together with a decrement of the quanta of the mirror's vibration mode and an increment of the photon number, or vice versa. Thus when initially the mirror is in vacuum and the atom is in the excited state, the total state cannot evolve to the 'dressed state", but only stays in the initial state accompanied by a dynamical phase factor.

The above-obtained results are very similar to that of the J–C model: $p_n(t)$ and $W(t)$ also contain many Rabi oscillations with various frequencies, and in different initial states, $p_n(t)$ and $W(t)$ behave differently.

Next we consider that the mirror is initially in a thermal state, while the photon field is in one of several different states: a thermal state, a Fock state $|n_0\rangle_a$ and a coherent state $|\alpha\rangle_a$. We obtain different initial parameters as follows:

$$\lambda^{\text{thermal}}_{ij;ij} = \frac{\mathrm{e}^{\beta\omega_0} - 1}{\mathrm{e}^{\beta\omega_0(i+1)}}\frac{\mathrm{e}^{\beta\omega_M} - 1}{\mathrm{e}^{\beta\omega_M(j+1)}}, \tag{51a}$$

$$\lambda^{\text{Fock}}_{ij;ij} = \delta_{in_0}\frac{\mathrm{e}^{\beta\omega_M} - 1}{\mathrm{e}^{\beta\omega_M(j+1)}}, \tag{51b}$$

$$\lambda^{\text{coherent}}_{ij;ij} = \exp\left(-|\alpha|^2\right)\frac{|\alpha|^{2i}}{i!}\frac{\mathrm{e}^{\beta\omega_M} - 1}{\mathrm{e}^{\beta\omega_M(j+1)}}, \tag{51c}$$

where $\beta = 1/k_BT$, and T is the temperature.

In figures 6, 7 and 8, we plot the evolution of $W(t)$ in the three initial states mentioned above with the parameters $T = 1$ K, $M = 10^{-10}$ kg, $l_0 = 1$ μm, $\omega_0 = \eta = 1.9 \times 10^{15}$ Hz, $\omega_e = \omega_0 - 0.999\omega_M$, $\omega_M = 10^9$ Hz, $n_0 = 10$, $\alpha = 10$. It can be seen from the figures that in each case, as time increases, collapses and revivals appear cyclically, but the time durations in which each collapse and each revival take place differ from each other because of different $\lambda_{ij;ij}$ that represent the weight of the Rabi oscillation with fixed frequency. This behaviour of collapse and revival of inversion is repeated with increasing time, with the amplitude of Rabi oscillations decreased and the time duration in which the revival takes place increased and ultimately overlapping with the earlier revival.

Note that the temperature is so low that $\left[\exp(\beta\omega_0) - 1\right]/\exp\left[\beta\omega_0(\mathrm{i}+1)\right] \to \delta_{i0}$, and thus the case described in figure 6 reflects the phenomenon that the atomic transition between the upper and the lower level can happen even when the light field is initially prepared in the vacuum state. This is obviously a purely quantum effect to prove the role of vacuum. In figure 7, we observe that even in the cavity field in a Fock state, the collapse and revival appear explicitly. This case differs from the J–C model based collapse and revival phenomenon, in which the evolution of inversion is just a cosine curve when the field is in a Fock state.

7. Conclusion and remarks

We have shown a AAOPM coupling in the triple hybrid system composing of atoms, a cavity field and a movable mirror and discovered that under the parametric resonance condition, this complicated model can be solved exactly. Furthermore, we have demonstrated that this triple hybrid system can be modelled by generalized *L–S* coupling under the rotating-wave approximation under the frequency resonance condition. It is shown that the composite object formed by the cavity-field-dressed mirror acts like an orbital angular momentum.

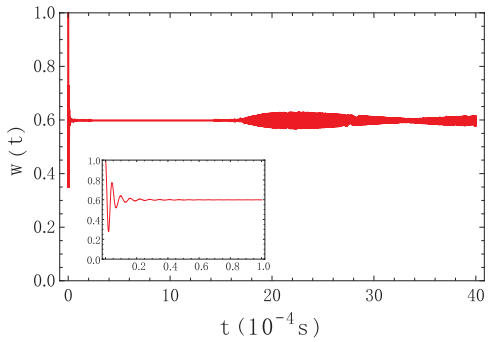

Figure 6. Time evolution of the population inversion $W(t)$ for an initially thermal state for both the cavity field and the mirror.

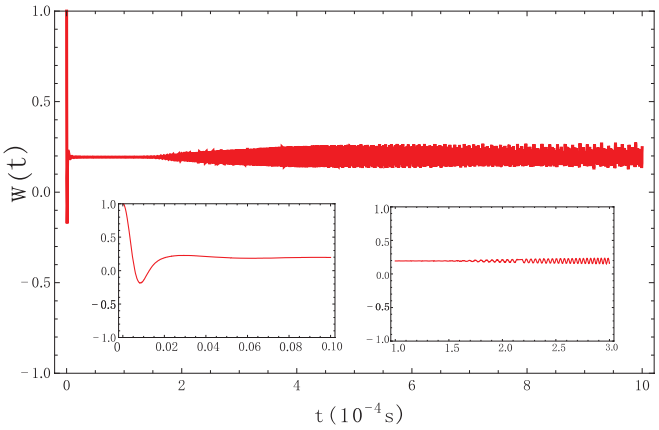

Figure 7. Time evolution of the population inversion $W(t)$ for an initially thermal state for mirror and a Fock state $|n_0\rangle_a$ for the field with $n_0 = 10$.

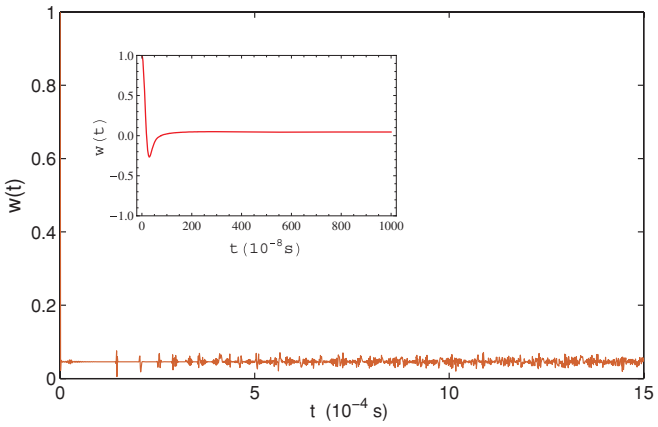

Figure 8. Time evolution of the population inversion $W(t)$ for an initially thermal state for the mirror and a coherent state $|\alpha\rangle_a$ for the field with $\alpha = 10$.

Then we studied the physically intrinsic relation between the generalized *L–S* coupling system and the J–C model, i.e., when the orbital angular momentum is large enough, the former is quite like the latter. Similarly to the generalized *L–S* coupling system, in the quasi-classical limit, the ladder operators behave as the bosonic operators and thus the large angular momentum can be regarded as 'excitons' in the low excitation limit. We also investigated some characteristic properties of the J–C model in our triple hybrid system and discovered their similarities and differences.

Acknowledgments

C P Sun acknowledges support by the NSFC with grants no 10474104, no 60433050 and no 10704023, NFRPCNo 2006CB921205 and 2005CB724508.

Appendix A. Calculation of η'

In this appendix, we give the details for deriving η', which the triple coupling strength is proportional to.

We consider the atom fixed at x_0 in the cavity, and then we do not consider the motion of the mass-center of the atom. As a consequence, we just need to consider how the oscillating mirror influences the electric field E and the atom–cavity coupling strength via the change of the cavity length l. Note that

$$E(x_0) = \sqrt{k/\epsilon_0 V}\, a \sin(kx_0) + \text{h.c.},$$

where ϵ_0 is the dielectric constant in vacuum. Here, $k = 2\pi/l$ is the wavenumber of the cavity field and $V \propto l$ is the cavity volume, both of which depend on the cavity length. When l varies from l_0 to $l_0 + x$, where x is the displacement of the mirror, expanding the term $\sqrt{k/\epsilon_0 V}\sin kx_0$ to the first order of x leads to

$$E(x_0) \approx \epsilon_0 a \sin(k_0 x_0) - [\sin(k_0 x_0) + k_0 x_0 \cos(k_0 x_0)]\,\epsilon_0 a \frac{x}{l_0} + \text{h.c.}$$

Here,

$$k_0 = 2\pi/l_0,$$

$$\epsilon_0 = \sqrt{k_0/\epsilon_0 V_0},$$

where V_0 is the cavity volume when the cavity length is l_0.

For convenience, we take out the subscript '0' of k_0, ε_0 and l_0. Then we obtain equation (2) and η' with the form

$$\eta' = (\sin kx_0 + kx_0 \cos kx_0)\,\varepsilon/l.$$

References

[1] Genes C, Vitali D and Tombesi P 2008 *Phys. Rev.* A **77** 050307
[2] Meiser D and Meystre P 2006 *Phys. Rev.* A **73** 033417
[3] Ian H, Gong Z R, Liu Y-X, Sun C P and Nori F 2008 *Phys. Rev.* A **78** 013824
[4] Vitali D, Gigan S, Ferreira A, Böhm H R, Tombesi P, Guerreiro A, Vedral V, Zeilinger A and Aspelmeyer M 2007 *Phys. Rev. Lett.* **98** 030405
[5] Marshall W, Simon C, Penrose R and Bouwmeester D 2003 *Phys. Rev. Lett.* **91** 130401
[6] Bose S, Jacobs K and Knight P L 1999 *Phys. Rev.* A **59** 3204–10
[7] Mancini S and Tombesi P 1994 *Phys. Rev.* A **49** 4055
[8] Yi X X, Sun H Y and Wang L C 2008 arXiv:0807.2703
[9] Zhang P, Wang Y D and Sun C P 2005 *Phys. Rev. Lett.* **95** 097204

[10] Mancini S, Giovannetti V, Vitali D and Tombesi P 2002 *Phys. Rev. Lett.* **88** 120401
[11] Gong Z R, Ian H, Liu Y-X, Sun C P and Nori F 2008 arXiv:0805.4102
[12] Bhattacharya M and Meystre P 2007 *Phys. Rev. Lett.* **99** 073601
[13] Zhang P, Liu X F and Sun C P 2002 *Phys. Rev.* A **66** 042104
[14] Quan H T, Song Z, Liu X F, Zanardi P and Sun C P 2006 *Phys. Rev. Lett.* **96** 140604
[15] Sun C P 1993 *Phys. Rev.* A **48** 898
[16] Liu Y X, Imoto N, Özdemir Ş K, Jin G R and Sun C P 2002 *Phys. Rev.* A **65** 023805
[17] Jin G R, Zhang P, Liu Y-X and Sun C P 2003 *Phys. Rev.* B **68** 134301
[18] Sun C P, Li Y and Liu X F 2003 *Phys. Rev. Lett.* **91** 147903
[19] Li Y and Sun C P 2004 *Phys. Rev.* A **69** 051802
[20] He L, Liu Y X, Yi S, Sun C P and Nori F 2007 *Phys. Rev.* A **75** 063818
[21] Landau L D and Lifshitz E M 1977 *Quantum Mechanics (Non-relativistic Theory)* 3rd edn (Oxford: Butterworth-Heinemann)
[22] Sakurai J J 1994 *Modern Quantum Mechanics* (Reading, MA: Addison-Wesley)
[23] Meiser D and Meystre P 2006 *Phys. Rev.* A **74** 065801
[24] Ciuti C and Carusotto I 2006 *Phys. Rev.* A **74** 033811
[25] Plumridge J, Clarke E, Murray R and Phillips C 2008 *Solid State Commun.* **146** 406
[26] Bose S, Jacobs K and Knight P L 1997 *Phys. Rev.* A **56** 4175
[27] Arcizet O, Cohadon P-F, Briant T, Pinard M, Heidmann A, Mackowski J-M, Michel C, Pinard L, Francais O and Rousseau L 2006 *Phys. Rev. Lett.* **97** 133601
[28] Arcizet O, Briant T, Heidmann A and Pinard M 2006 *Phys. Rev.* A **73** 033819
[29] Orszag M 2000 *Quantum Optics: Including Noise Reduction, Trapped Ions, Quantum Trajectories and Decoherence* (Berlin: Springer)